

## List of Contents

| S No. | Content  | Page No. |
|-------|--|----------|
|       | Abstract   |          |
| 1.    | Introduction   | 11       |
| 1.1.  | OCEANSAT-1 ocean colour monitor (OCM-1)                              | 11       |
| 1.2.  | Specifications of OCM-1  | 11       |
| 1.3.  | OCM-1 coverage over North Indian Ocean                               | 12       |
| 1.4.  | Data format and file naming conventions                              | 14       |
| 2.    | Generation of geophysical products                                   | 15       |
| 2.1.  | SeaWiFS Data Analysis System (SeaDAS)                                | 16       |
| 2.2.  | Data processing from level-1B to level-2                             | 16       |
| 2.3.  | Atmospheric correction methodology for OCM-1                         | 17       |
| 2.4.  | Data Processing from level-2 to level-3                              | 20       |
| 2.5.  | Algorithm for chlorophyll-a concentration (OC2, OC4)                 | 21       |
| 2.6.  | Diffuse attenuation coefficient ( $K_d_{490 \text{ nm}}$ ) algorithm | 23       |
| 3.    | Validation of OCM-1 chlorophyll-a concentration                      | 24       |
| 3.1.  | SeaBASS Archive  | 24       |
| 3.2.  | Validation of OCM-1 Chlorophyll-a Concentration with SeaBASS         | 24       |
| 4.    | Future scope of the work   | 27       |
| 5.    | References   | 28       |
|       | Appendix-I   | 30       |
|       | Appendix-II  | 34       |



## List of Figures

- Figure 1:** OCM-1 passes coverage over the Indian ocean
- Figure 2:** Representation of the North Indian Ocean based on the ocean bathymetry map of 0 to 6 km depth
- Figure 3:** OCM-1 TOA radiance RGB image on 6<sup>th</sup> January 2000 pass number 010 and row number 013
- Figure 4:** Illustration of light interaction with the atmosphere, sea surface and reaching to the sensor
- Figure 5:** OCM-1 atmospheric correction flow chart from TOA radiance to geophysical product generation.
- Figure 6:** OCM-1 processing flow chart from L1B to data dissemination through NICES Bhuvan\_web portal
- Figure 7:** OCM-1 chlorophyll (OC2, mg/m<sup>3</sup>) map 2-day composite on 7 and 8 of January 2000
- Figure 8:** OCM-1 chlorophyll (OC4, mg/m<sup>3</sup>) map 2-day composite on 7 and 8 of January 2000
- Figure 9:** OCM-1 diffuse attenuation coefficient ( $kd_{490}$ , /m) map 2-day composite on 7 and 8 of January 2000
- Figure 10:** November 2001 MIPOT cruise track coverage over Indian ocean from SeaBASS archive
- Figure 11:** Ship track of MIPOT cruise imported on monthly chlorophyll (OC4) concentration (mg/m<sup>3</sup>) in November 2001 at 9 km resolution, the black line is showing the ship track.
- Figure 12:** Correlative plot between in-situ chlorophyll-a and OCM-1 monthly OC2 chlorophyll in linear scale (top left) and logarithmic scale (top right) and OCM-1 OC4 chlorophyll in linear scale (bottom left) and logarithmic scale (bottom right) on November 2001.
- Figure 13:** Correlative plot between in-situ chlorophyll-a with OCM-1 level-2 OC2 chlorophyll-a (left) and OCM-1 OC4 chlorophyll-a (right) respectively on 23 November 2001.

## **List of Tables**

**Table 1:** *Oceansat-1 Ocean colour Monitor sensor specifications*

**Table 2:** *Meteorological parameters and role in atmospheric correction along with their temporal and spatial resolution used in SeaDAS data processing*

**Table 3:** *Maximum chlorophyll ratio and OCM-1 chlorophyll algorithm coefficients for OC4 algorithm*

**Table 4:** *Maximum Rrs ratio and OCM-1 algorithm coefficients for the Kd\_490 nm algorithm.*

**Table 5:** *Number of in-situ MIPOT cruise stations covered in the North Indian Ocean.*

**Table 6:** *Statistics showing the validation results of SeaBASS ins-situ data with OCM-1 chlorophyll concentration.*

## **Abstract**

OCEANSAT-1 ocean colour monitor (OCM-1), an historical ocean colour sensor from the Indian Space Research Organization (ISRO) operated from 1999 to 2010. OCM-1 was designed to address various ocean colour applications such as identification of potential fishing zones (PFZs) one of the applications, also to study the ocean biogeochemical cycles, aerosol studies, dust plume identification, harmful algal blooms monitoring, etc. A total of eleven years of geophysical products from 1999 to 2010 were processed to create climate quality data records to study long-term biological variability over the North Indian Ocean (NIO). The processed geophysical products were hosted on the National Information System for Climate and Environmental Studies (NICES) web-portal. This technical report describes the processing levels involved from level-1B to level-3, atmospheric correction methodology adopted, and validation of the chlorophyll-a product. The products retrieved from OCM-1 are chlorophyll-a concentration (chl-a in mg/m<sup>3</sup>), diffuse attenuation coefficient ( $K_d_{490}$  nm, in /m) at 1 km spatial resolution, and temporal resolution at 2-day, 8-day, and monthly. Long term biological studies and atmospheric processes are possible by combining OCM-1 & 2 based on appropriate normalization.

## **Acknowledgments**

This study was carried under the National Information System for Climate and Environmental Studies (NICES) program. We thank NRSC Data Processing Area for providing OCM-1 L1B radiometrically calibrated data. We thank K. H. Rao, Former Scientist, NRSC for his guidance and encouragement towards the work carried out. We thank NASA Goddard Space Flight Center, Ocean Biology Processing Group (NASA, OBPG) for providing SeaWiFS chlorophyll data and SeaDAS software for processing. We thank Gnuplot version 5.0 (command-line tool) used for visualization and statistics of data.



# 1. Introduction

## 1.1. OCEANSAT-1 ocean colour monitor (OCM-1)

Ocean colour monitor onboard OCEANSAT-1 (OCM-1) is the first instrument to take advantage of push-broom technology for achieving higher radiometric performance and higher spatial resolution by maintaining a large swath to provide high revisit time for ocean observations. The instrument design is an extension of the imaging concept adopted for Indian Remote Sensing (IRS) Linear Imaging Self Scanning System (LISS) payloads (Navalgund and Kiran Kumar, 1999).

The IRS-P4 OCM data would be extremely useful for the estimation of phytoplankton in oceanic/coastal waters, detection and monitoring of phytoplankton blooms, coastal upwelling, suspended sediment dynamics, identification of water mass boundaries, and oil pollution. The information on pigments, in conjunction with sea surface temperature, will greatly assist in the identification of potential fishery zones in coastal and oceanic waters (Solanki and Dwivedi, 2003). IRS-P4 OCM, along with other contemporary ocean colour sensors such as IRS-P3 Modular Optoelectronic Scanner (MOS), Sea-viewing Wide Field-of-view Sensor (SeaWiFS), Medium Resolution Imaging Spectrometer (MERIS), and Moderate Resolution Imaging Spectrometer (MODIS) will assist the global ocean colour community in filling data gaps by data merging methods, and can also be used for the inter-calibration of different ocean colour sensors (Navalgund and Kiran Kumar, 1999).

To observe long term ocean biological changes and continue the fisheries applications OCEANSAT-2 Ocean colour Monitor (OCM-2) was launched in September 2009 (Navalgund and Chauhan, 2009), OCM-3 an ocean colour sensor similar to OCM-1 & 2 planned to be launched in 2020. OCM-1 spectral bands are chosen to retrieve low to high chlorophyll concentration. With the improved high spatial resolution, inland water bodies studies are possible with OCM-1. The native resolution of OCM-1 is capable of distinguishing coastal and land areas compared to existing typical 1-km sensors.

## 1.2. Specifications of OCM-1

Oceansat-1 Ocean colour Monitor (OCM-1) was launched in May 1999, and data is available for the users from June 1999 after successful satellite maneuvers. OCM-1 orbited in a polar sun-synchronous orbit at 720 km altitude. Scanned the Earth at 360 m across-track resolution and 236 m along-track resolution at nadir. Equatorial crossing time was 12:30 hours, revisiting time was 2 days for NIO made possible with a wide swath 1420 km. OCM-1 is a scanning radiometer that measures the radiance in

Visible and NIR wavelengths. It measures the reflected radiance from the Earth using Charge-Coupled Devices (CCD) detectors. 6000 detectors are mounted on one strip of OCM-1 camera per one wavelength, out of these 3730 detectors are calibrated to detect the top of the atmosphere (TOA) radiance. Signal to Noise Ratio values and other information mentioned in **Table 1**. The instrument is facilitated to provide tilt in the along-track direction to avoid sun glint.

**Table 1:** Oceansat-1 Ocean colour Monitor sensor specifications

|                                      | <b>Ocean colour Monitor-1</b>     |                                    |                                 |
|--------------------------------------|-----------------------------------|------------------------------------|---------------------------------|
| <b>Launch data</b>                   | 26 May 1999                       |                                    |                                 |
| <b>Orbit type</b>                    | polar sun-synchronous at 720 km   |                                    |                                 |
| <b>Equator crossing</b>              | 12 noon $\pm$ 20 min, descending  |                                    |                                 |
| <b>Orbital period</b>                | 99.31 min                         |                                    |                                 |
| <b>Swath width</b>                   | 1420 km                           |                                    |                                 |
| <b>Spatial resolution (at nadir)</b> | 360 x 236 m                       |                                    |                                 |
| <b>Real-time data rate</b>           | 21299.2 Kbps (20.8 Mb/s)          |                                    |                                 |
| <b>Transmitted frequency</b>         | X-band                            |                                    |                                 |
| <b>Revisit time</b>                  | 2 days                            |                                    |                                 |
| <b>Digitization</b>                  | 12 bit                            |                                    |                                 |
| <b>Operation period</b>              | 02/06/1999 to 08/08/2010          |                                    |                                 |
|                                      | <b><math>\lambda</math> in nm</b> | <b>SNR(<math>L_{typ}</math>) *</b> | <b>NE<math>\Delta</math>L *</b> |
| <b>Band 1:</b>                       | 404-423                           | 340.5(9.1)                         | 0.026                           |
| <b>Band 2:</b>                       | 431-451                           | 440.7(8.4)                         | 0.019                           |
| <b>Band 3:</b>                       | 475-495                           | 427.6(6.6)                         | 0.015                           |
| <b>Band 4:</b>                       | 501-520                           | 408.8(5.6)                         | 0.014                           |
| <b>Band 5:</b>                       | 547-565                           | 412.2(4.6)                         | 0.011                           |
| <b>Band 6:</b>                       | 660-677                           | 345.6(2.5)                         | 0.0072                          |
| <b>Band 7:</b>                       | 749-787                           | 393.7(1.6)                         | 0.004                           |
| <b>Band 8:</b>                       | 847-882                           | 253.6(1.1)                         | 0.004                           |

\* in (mW/cm<sup>2</sup>/um/sr) units

Noise Equivalent Radiance (NE $\Delta$ L) =  $L_{typ}/SNR$



### 1.3. OCM-1 coverage over the North Indian ocean

OCM-1 high spatial resolution (360 m) made it possible to study coastal biological processes such as harmful algal blooms, aerosol studies, dust plume identifications over the North Indian ocean (Longitude from 50 ° to 100 ° E, Latitude from 0 ° to 30 ° N, the average depth of NIO is ~ 3500 m). OCM-1 covers the North Indian ocean termed as local area coverage (LAC) on alternative days. To maintain ease of handling the data, OCM-1 coverage is available with path and row numbers, specific regions over the Indian ocean shown in **Figure 1**. Path numbers indicate vertical coverage (for example 008, 009, 010, 011), and row indicates horizontal coverage (for example 013, 014, 015).

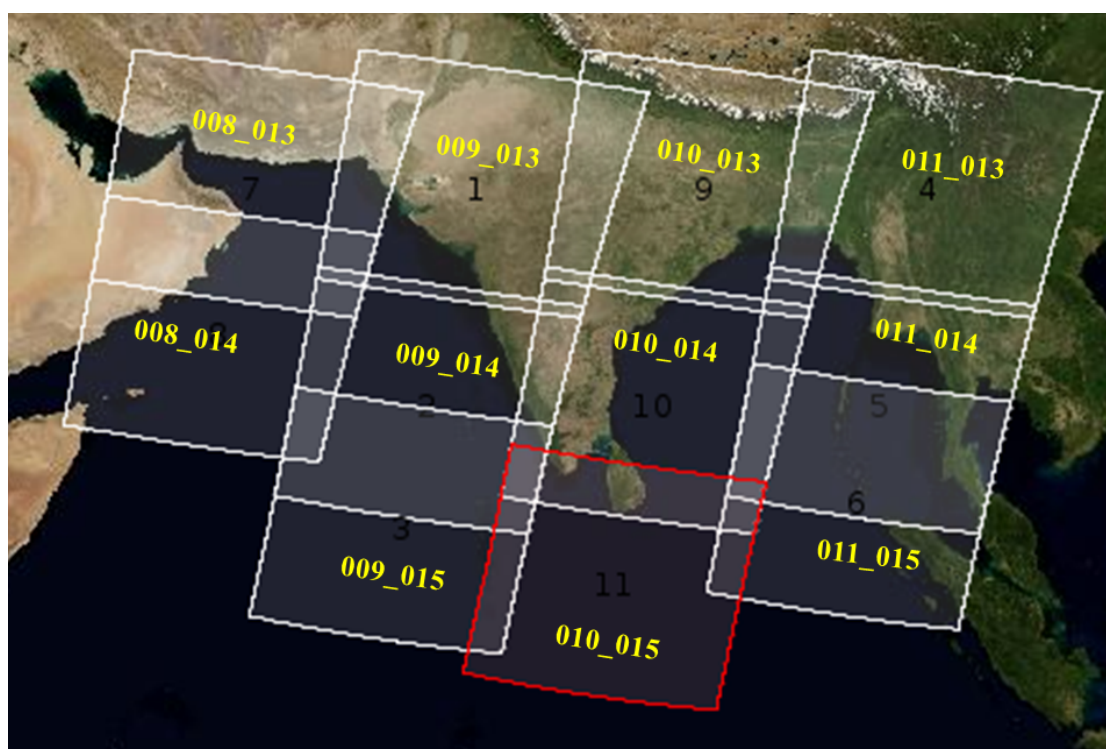


**Figure 1:** OCM-1 passes coverage over the Indian ocean

Bathymetry plays an important role in the sensor measured reflectance spectra in areas with very shallow waters, below 15 to 20 meters depending on water clarity. The bathymetry map on NIO is shown in **Figure 2**. Shallow waters contribute to the bottom effect which may not be the intended signal from the water column exactly. During the atmospheric correction process of OCM-1 in the SeaDAS package processing identifies shallow water as a *COASTZ* flag. Water classes are based on depth, useful to evaluate algorithm performance, and analyze uncertainties in atmospheric correction over open or coastal waters. Since, depth from 0 to 200 m and 200 m to 5000 m for the North Indian Ocean produced in **Figure A1, A2**.

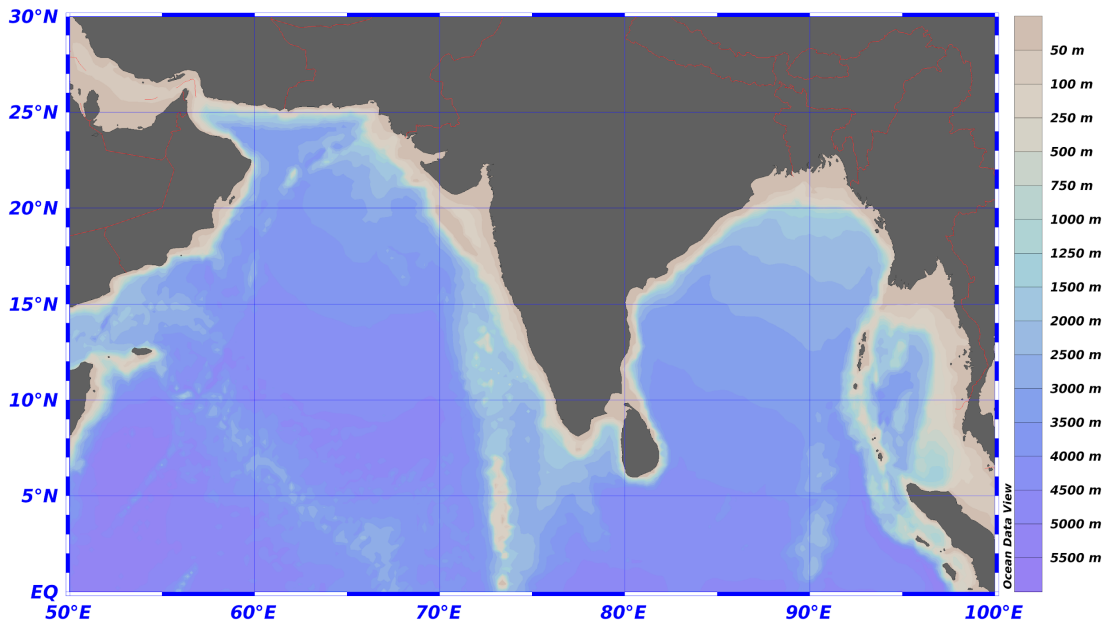


**Figure 2:** Representation of the North Indian Ocean based on the ocean bathymetry map of 0 to 6 km depth

#### 1.4. Data format and file naming conventions

In the atmospheric correction (l2gen) procedure OCM-1 L1B data is input. L1B file name contains the date of acquisition, path and row information, number of scan lines and pixels. Sample OCM-1 red green and blue (RGB) image shown in **Figure 3**, useful for initial identification of cloud presence and haziness in visible imagery.

*Input L-1B sample file*

I2000001081138\_008\_013\_6610\_3730\_L1B\_OCM1.hdf

For a sample L1B file, the first character 'I' stands for IRS, two to five characters indicates the year (2000), the next three characters indicate Julian day (001), the next six characters indicates time of acquisition (081138), and followed by a path (008), row (013), number of scan lines (6610), number of pixels (3730) and sensor name (OCM1).

OCM-1 final output files which are distributed through the NICES portal in NetCDF format along with image file (png file). Output NetCDF file name includes the date of acquisition in Julian day convention, spatial and temporal resolution, geophysical product algorithm.

*Output NetCDF file name available in NICES portal*

**2 Day :** SMI\_1KM\_OC4\_001\_002\_2000\_2D.nc

**8 Day :** SMI\_1KM\_OC4\_001\_008\_2000\_8D.nc

**Monthly** : SMI\_1KM\_OC4\_JAN\_2000.nc

*Output Image file name available in NICES portal*

**2 Day** : SMI\_1KM\_OC4\_001\_002\_2000\_2D.png

**8 Day** : SMI\_1KM\_OC4\_001\_008\_2000\_8D.png

**Monthly** : SMI\_1KM\_OC2\_JAN\_2000\_CB.png

Network Common Data Format (NetCDF / .nc) is designed to support different types of operating systems, compatible to store raster data in arrays. Auxiliary information about the data, such as what units are used (metadata), is stored with the data.

### ***Metadata***

netCDF file is available with metadata containing information about sensor and processing options. Metadata of a file is stored as global attributes, metadata of a variable or scientific data set is stored as variable attributes. Few attributes are mentioned in **Table A1**.

Variable attributes give information about units of the variable, scale factor, and offset to convert scaled integers to floating-point numbers if the variable is stored as an integer. Also, the valid minimum and maximum of the variable fill value replaces the pixel when data is not available, as shown in **Table A2**. Different levels involved in the ocean colour data processing scheme explained at <https://oceancolour.gsfc.nasa.gov/products/>.

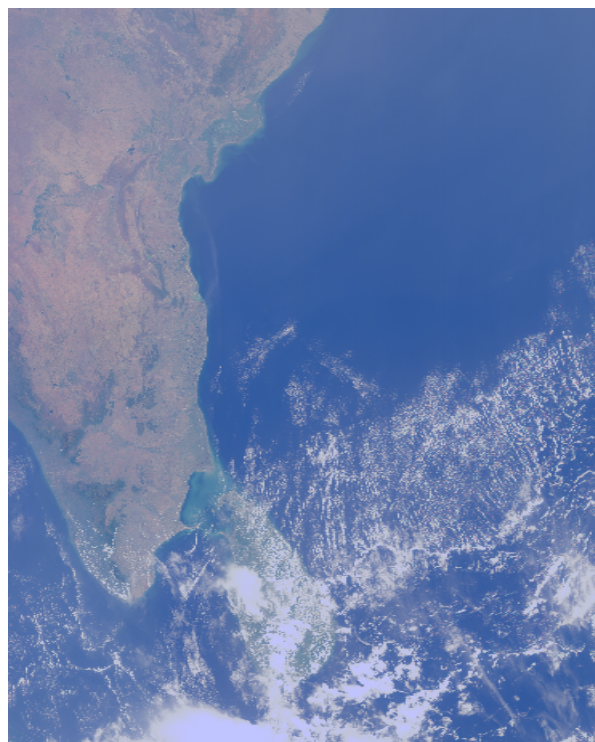


**Figure 3:** OCM-1 TOA radiance RGB image on 6<sup>th</sup> January 2000 pass number 010 and row number 013.

## 2. Generation of geophysical products

One of the main objectives of OCM-1 is the generation of geophysical products such as chlorophyll-a concentration, diffuse attenuation coefficient, to create a long term climate quality database under the NICES program to address various scientific problems related to climate change. NICES is a platform that hosts essential climate variables (ECVs) for long term climate studies for land, ocean, and atmosphere. To maintain consistency over global ocean colour products for OCM-1, SeaDAS processing software was used from atmospheric correction (level -2) to spatial maps generation (level -3).

### 2.1. SeaWiFS Data Analysis System (SeaDAS)

OCM-1 entire mission data from 1999 to 2010 were processed using the SeaWiFS Data Analysis System (SeaDAS) software. SeaDAS is an open-source software package for processing, analysis, and display of ocean colour remote sensing measurements from a variety of satellite-based multispectral radiometers from different space agencies distributed by Ocean Biology Processing Group / National Aeronautics and Space Administration. SeaDAS provides different modules in the processing chain like *l2gen*, *l2bin*, *l3bin*, and *smigen*, etc, (<https://seadas.gsfc.nasa.gov>). SeaDAS has been customized for the OCM-1 sensor by considering sensor-specific information and other calibration files. Lookup tables provided for the correction of Rayleigh radiance and aerosol radiance by considering sensor specifications depending upon a suitable vector radiative transfer model.

### 2.2. Data processing from level-1B to level-2

Processed chlorophyll-a concentration (OC2, OC4) and diffuse attenuation coefficient ( $K_d_{490}$  nm) from OCM-1 radiometrically corrected TOA (L1B) data using multi-sensor level-1 to level-2 module (*l2gen* version 8.10.3-r0) in SeaDAS software at sensor native resolution (360 m). *l2gen* processing thresholds (cloud, glint threshold, aerosol options, and maximum wind speed mentioned in **Table A4**) adopted from NASA/OBPG.

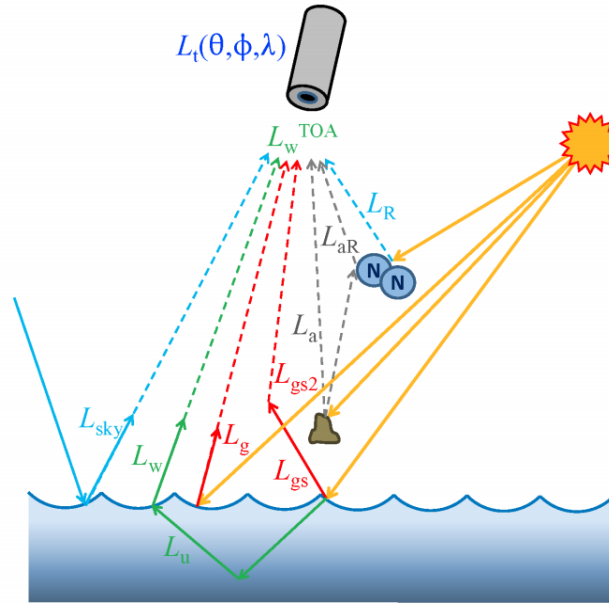


**Figure 4:** Illustration of light interaction with the atmosphere, sea surface and reaching to the sensor (*source: Mobley et al 2016*)

### 2.3. Atmospheric Correction Methodology for OCM-1

To retrieve any geophysical product from the sensor measured TOA radiance ( $L_t$ ), atmospheric contribution needs to be removed (Gordon et al 1997, IOCCG-10). In  $L_t$ , typically 90% of radiance is from path radiance which includes molecular scattering (Rayleigh), aerosol scattering (single scattering), and an interaction term between molecules and aerosols (multiple scattering) (Andre et al 1991). Different radiances contributing to TOA are represented in **Figure 4**. Water is highly absorptive in nature and only 20 % or less of the total signal is from water (Hovis et al 1977). TOA Rayleigh radiance ( $L_r$ ) is highly dominated which contributes 88 %, 83 %, 78 %, 69 %, 59 %, and 50 % in 412 nm, 443 nm, 490 nm, 555 nm, 670 nm, and 765 nm respectively (Wang et al 2016) in  $L_t$  since  $L_r$  needs to be computed accurately (Gordon et al 1994). Computation of  $L_r$  performed using Rayleigh Look Up Tables (LUTs) developed by iterative radiative transfer code (Ahmad et al 1982). Rayleigh LUTs are functions of Rayleigh optical thickness ( $\tau_R$ ), sensor and solar geometry (sensor, solar zenith angles, and relative azimuth angles), and sigma of wind speed. Pressure correction needs to be applied to  $\tau_R$  for accounting dependency of the relation between the number of molecules and sea level pressure at the time of measurement (Gordon et al 1988, Wang et al 2005). A parameter sigma of wind speed (a function of wind speed) was incorporated in Rayleigh LUTs to characterize surface roughness impact on Rayleigh radiance (Wang et al 2002). The critical component in atmospheric correction is aerosol quantification and it's a correction due to its dynamic spatial and temporal variability. Aerosol radiance ( $L_a$ ) (single and multiple scattering) computed from two bands in NIR (765 nm and 865 nm) (Gordon et al

1994) based on black pixel assumption (Seigel et al 2000).  $L_a$  at visible bands computed using angstrom exponent (which is a function of  $L_a$  at NIR bands) by extrapolation method (Gordon et al 1994). A new suite of aerosol models is based on eight relative humidity and ten size fraction types (Ahmad et al 2010) used in the present study. Aerosol radiance LUTs are functions of scattering angles, angstrom exponent ( $\alpha$ ), extinction coefficient, phase function. Aerosol optical thickness ( $\tau_a$ ) computed by knowing the epsilon (a function of wavelength ratio and  $\alpha$ ) at the respective wavelength, therefore aerosol reflectance will be retrieved from AOT, phase function, and single scattering albedo (Gordon et al 1994).

Sun glint is a specularly reflected light that occurs, when the sun and sensor have similar geometry depending on the surface roughness. Normalized glint radiance ( $L_{GN}$ ) computed by considering solar, sensor geometry, and wind speed to account for the sea surface roughness. A threshold of 0.005 (/sr) and 0.0001 (/sr) for  $L_{GN}$  used to identify and mask the high glint and moderate glint respectively. Ocean colour products can be retrieved over the moderate glint pixels by removing the glint radiance (Wang and Bailey et al 2001). For cloud screening, using a threshold of 0.027 (2.7 %) upon Rayleigh corrected TOA reflectance ( $\rho_a$ ) at 865 nm (Robinson et al 2003, Wang et al 2006).  $\rho_a$  means combined radiance from aerosol and surface effects. Input extraterrestrial solar irradiance ( $F_0$ ) is adopted by accounting Sun and Earth geometry dependency (Thuillier et al 2003). The sequential flow to correct atmospheric contribution is shown in **Figure 5**.

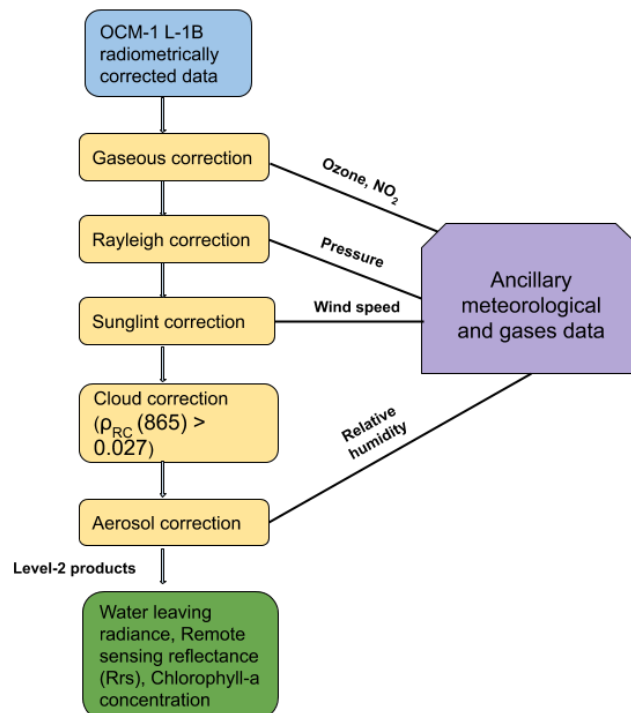


**Figure 5:** OCM-1 atmospheric correction flow chart from *TOA* radiance to geophysical products generation

As of now eight gases are considered globally (in the SeaDAS package) to carry out the atmospheric correction, which includes CO, CO<sub>2</sub>, N<sub>2</sub>O, NO<sub>2</sub>, O<sub>2</sub>, O<sub>3</sub>, CH<sub>4</sub>, H<sub>2</sub>O. Out of these CO, N<sub>2</sub>O, CH<sub>4</sub>, and CO<sub>2</sub> have negligible absorption at the Visible and Near Infrared (NIR) wavelengths. However, by appropriate selection of bands in the visible and NIR O<sub>2</sub>, O<sub>3</sub>, NO<sub>2</sub>, and H<sub>2</sub>O absorption can be accounted for (Mobley et al 2016). Among these, ozone is the dominant gas having high transmittance at green wavelengths. Specifically, OCM-1 chlorophyll (OC2, OC4) algorithms are based on remote sensing reflectance at 512 nm and 557 nm (O'Reilly et al 1998). Ozone contribution is less compared to Rayleigh and aerosol radiance, even though it should not be negligible. In general, an absorbing gas reduces the *TOA* radiance because the light is lost due to absorption. Correcting for this loss will increase the *TOA* radiance or reflectance (Mobley et al 2016). In OCRS, ozone absorption is only considered; the scattering of ozone is negligible due to its vertical distribution in the atmosphere (ozone presents a high concentration in the stratosphere compared to the troposphere) (Mobley et al 2016). NO<sub>2</sub> is generated by anthropogenic activities and occurs in both the troposphere and stratosphere, which attenuates light in blue wavelengths (Ahmad et al 2007).

**Table 2:** Meteorological parameters and role in atmospheric correction along with their temporal and spatial resolution used in SeaDAS data processing

| Meteorological parameter  | Present Source  | Role in atmospheric correction                                 |
|---------------------------|---|--|
| Atmospheric pressure (mb) | Monthly Climatology of 1997 to 2014 from NCEP (1x1 deg) | Rayleigh correction  |
| Relative Humidity (%)     |   | Selection of aerosol correction models                         |
| Wind speed (m/s)          |   | Rayleigh Lookup tables, sunglint radiance, white caps radiance |
| Ozone concentration (DU)  | Daily climatology of 2004 to 2013 OMI/TOMS(1x1 deg)     | Transmittance (significant in green wavelength)                |

|  |  |  |
|--|--|--|
| <b>NO<sub>2</sub> concentration (molecules / cm<sup>2</sup>)</b> | Monthly climatology of 2004 to 2013<br>from<br>SCIAMACHY/OMI/GOME<br>(0.25x0.25 deg) | Transmittance (significant in blue wavelength) |
|--|--|--|

In the computation of Rayleigh, aerosol, and glint radiances along with gases correction, few meteorological and atmospheric gases ancillary data are required. The spatial and temporal resolution of present ancillary sources is mentioned in **Table 2**.

#### 2.4. Data Processing from level-2 to level-3

Processed spatially binned products using ‘L2BIN’ (l2bin version 4.1.0) at day-wise and followed by temporally binned products at 2-day, 8-day, and monthly scale using ‘L3BIN’ (l3bin version 4.2.0) to improve pixel coverage despite cloud and sun glint presence at 1.20 km resolution. Generated standard mapped image (SMI) (smigen version 5.2.0) at 1 km resolution to maintain an equal spatial grid. Part of the processing, a group of quality checks assigned to each pixel in processing. Quality checks are two categories namely flags and masks, the flagged pixel will continue in the processing, but the pixel once masked will further remove from the processing. For example, if one pixel on the land surface will be flagged as a land mask, further removed in the processing. Thresholds (conditions) for different quality flags and their description furnished in **Table A5**.

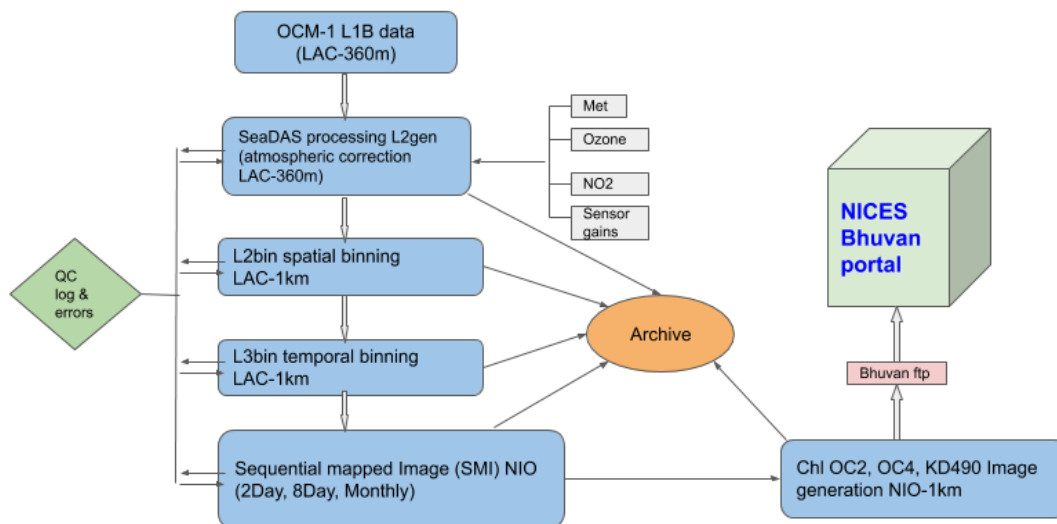


**Figure 6:** OCM-1 processing flow chart from L1B to data dissemination through Bhuvan\_web portal



The number of products processed at different levels from Level-1 to level-3 furnished in **Table A3**. A quality check took place at every level of processing. We identified an issue with *l2bin*, rectified by adding equatorial crossing time for the OCM-1 sensor in SeaDAS *l2bin* algorithm. Successfully generated 3485 days of geophysical products out of 4089 days of the total mission duration. Temporal binning of 2Day (1800), 8Day (468), and monthly (133) binned products were generated similar to OCM-2 products to maintain uniformity between both the sensors. Processing flow chart from L1B to product generation and hosting in the NICES portal shown in **Figure 6**.

## 2.5. Algorithm for chlorophyll-a concentration (OC2, OC4)

O'Reilly et al 1998 described, chlorophyll OC2 and OC4 algorithms are empirical relations derived from in-situ chlorophyll and remote sensing reflectance ( $R_{rs}$ ). Chlorophyll algorithms are fourth-degree polynomial equations whose input is  $R_{rs}$  at ocean colour bands. Specifically, OC2 uses  $R_{rs}$  ratio from two bands i.e.,  $R_{rs}$  (485 nm/ 556 nm), and OC4 uses four bands maximum ratio among  $R_{rs}$  (441 nm/ 556 nm),  $R_{rs}$  (485 nm/ 556 nm), and  $R_{rs}$  (510 nm/ 556 nm). Mathematical expression for OC2, OC4 shown below.

$$\log_{10}(Chl - a) = a_0 + \sum_{i=1}^4 a_i \left( \log_{10} \left( \frac{R_{rs}(\lambda_{blue})}{R_{rs}(\lambda_{green})} \right) \right)^i$$

where the numerator  $R_{rs}(\lambda_{blue})$ , is the greatest of several input  $R_{rs}$  values in blue bands concerning  $R_{rs}$  at the green band. OCM-1 blue band's central wavelengths are 441 nm, 485 nm, 510 nm, and the green band is 556 nm and  $a_0$ - $a_4$  are OCM-1 sensor-specific algorithm coefficients provided in SeaDAS as shown in **Table 3**. Retrieved OCM-1 chlorophyll 2-day composite images by using above OC2 and OC4 algorithms shown in **Figures 7 and 8**.

**Table 3:** Maximum remote sensing reflectance ratio and OCM-1 chlorophyll algorithm coefficients for OC4 algorithm

| Algorithm name               | $R_{rs}$ ratio            | $a_0$  | $a_1$   | $a_2$  | $a_3$   | $a_4$   |
|------------------------------|---------------------------|--------|---------|--------|---------|---------|
| OC2 ( $\frac{blue}{green}$ ) | $\frac{485}{555}$         | 0.2511 | -2.0853 | 1.5035 | -3.1747 | 0.3383  |
| OC4 ( $\frac{blue}{green}$ ) | $\frac{441>485>510}{555}$ | 0.3272 | -2.9940 | 2.7218 | -1.2259 | -0.5683 |

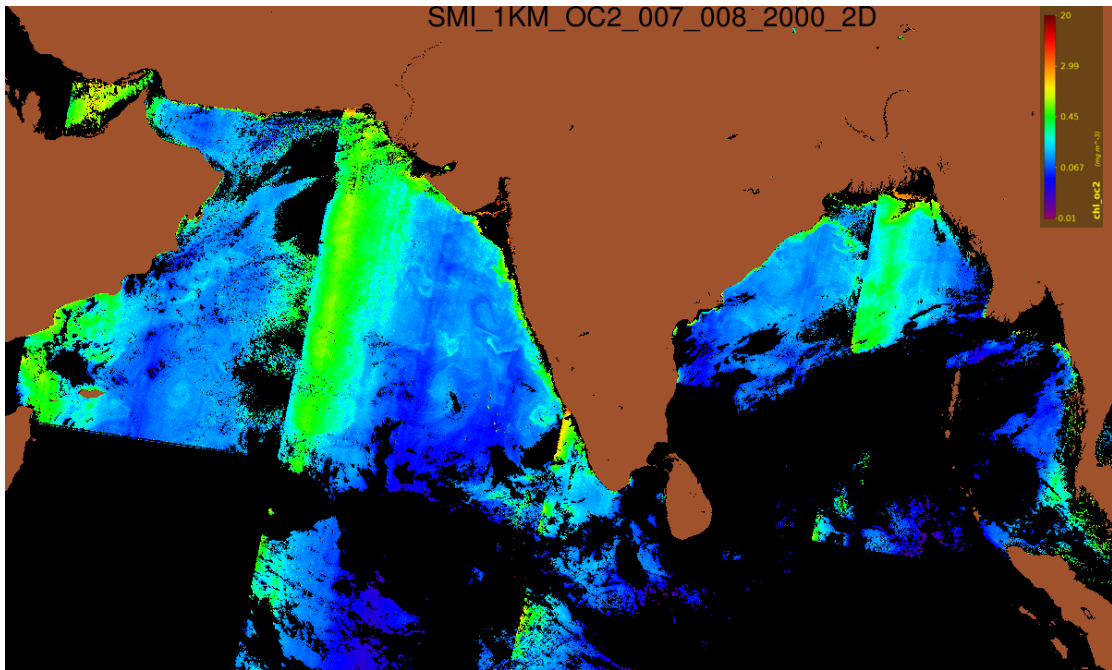


**Figure 7:** OCM-1 chlorophyll (OC2,  $\text{mg}/\text{m}^3$ ) map 2-day composite on 7 and 8 of January 2000

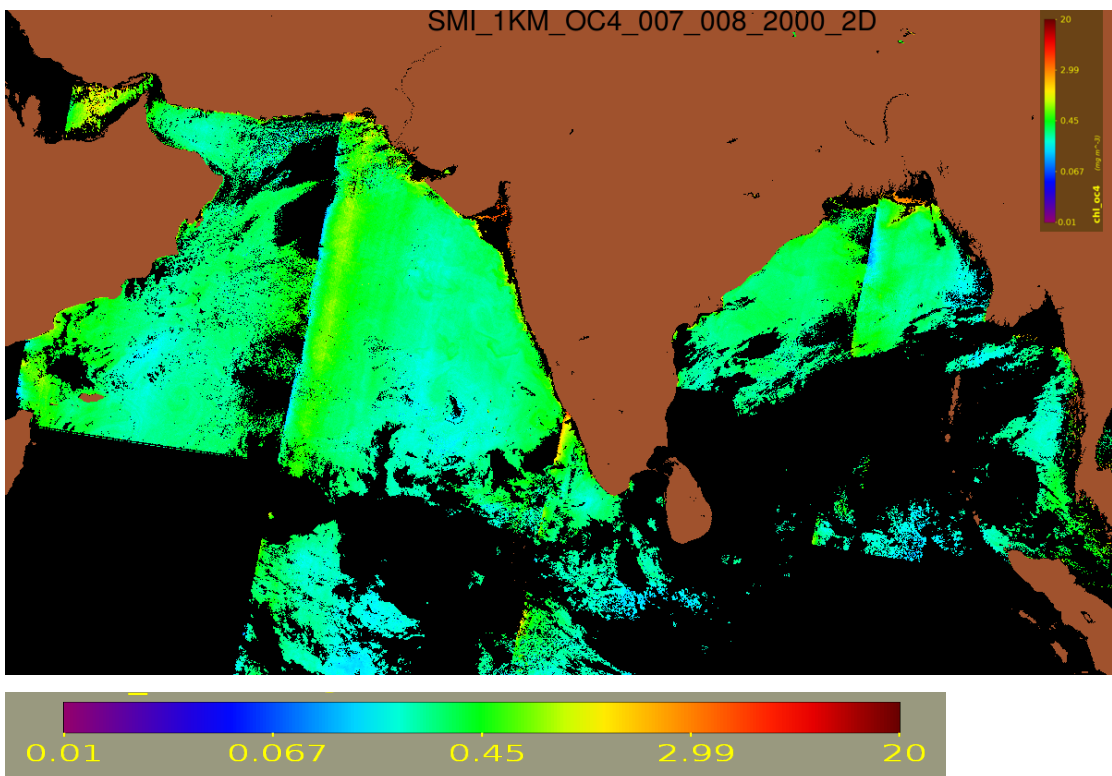


**Figure 8:** OCM-1 chlorophyll (OC4,  $\text{mg}/\text{m}^3$ ) map 2-day composite on 7 and 8 of January 2000

## 2.6. Diffuse attenuation coefficient ( $Kd_{490}$ nm)

In the water column, light energy and direction changes with depth, diffuse attenuation coefficient ( $Kd_{490}$  nm) is an optical property which describes the rate of change in light (downwelling irradiance) with depth. This parameter  $Kd_{490}$  nm is an indicator for turbidity or transparency of the water body, generally varies from 0 to 0.05 (/m) in open ocean waters shown in OCM-1  $Kd_{490}$  nm spatial map (Figure 9). The algorithm for  $Kd_{490}$  is a fourth-order polynomial relationship between a ratio of Rrs, also based on an empirical relation similar to the chlorophyll. OCM-1 algorithm coefficients are mentioned in Table 4.

$$\log_{10}(K_{bio}(490)) = a_0 + \sum_{i=1}^4 a_i \left( \log_{10} \left( \frac{R_{rs}(\lambda_{blue})}{R_{rs}(\lambda_{green})} \right) \right)^i$$

$$Kd_{490} = K_{bio}(490) + 0.0166$$

**Table 4:** Maximum Rrs ratio and OCM-1 algorithm coefficients for the  $Kd_{490}$  nm algorithm.

| Sensor | Rrs ratio             | $a_0$   | $a_1$   | $a_2$  | $a_3$   | $a_4$   |
|--------|-----------------------|---------|---------|--------|---------|---------|
| OCM-1  | $\frac{485>510}{555}$ | -0.8515 | -1.8263 | 1.8714 | -2.4414 | -1.0690 |

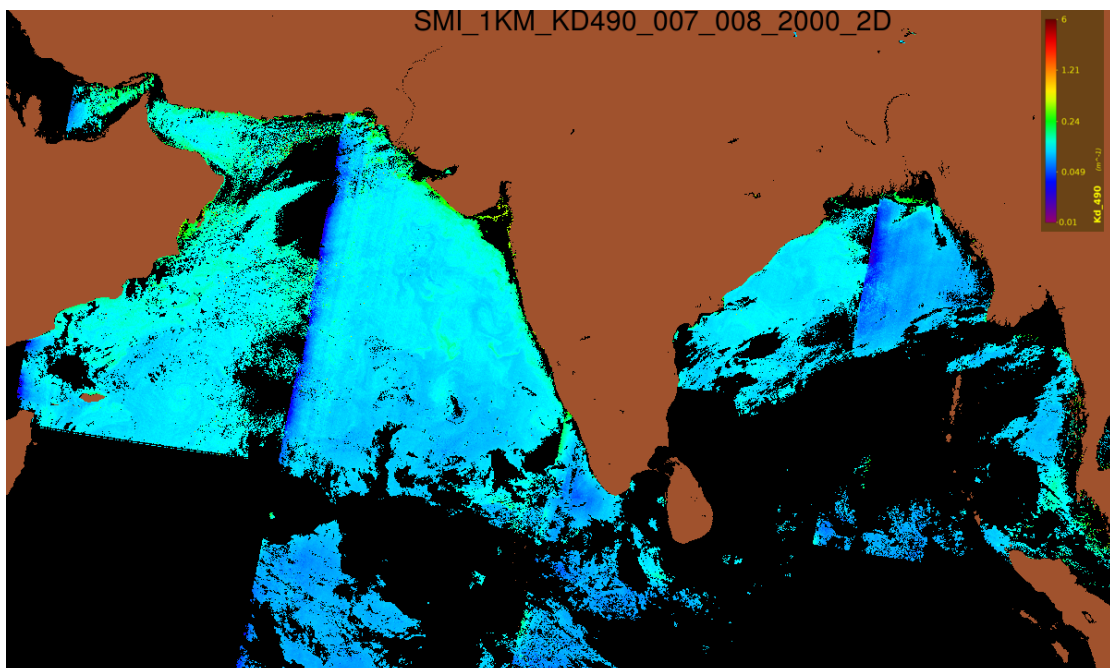


**Figure 9:** OCM-1 diffuse attenuation coefficient ( $kd_{490}$  in /m) map 2-day composite on 7 and 8 of January 2000

### 3. Validation of OCM-1 chlorophyll-a concentration

To ensure accurate product quality of global ocean optical, biological, and biogeochemical properties efforts are required to calibration and validation of the product (Mikelsons et al 2019, Barens et al 2019). Deriving global ocean colour data from space-based measurements is a very complicated and challenging task, which requires close attention to instrument calibration (including vicarious calibration), algorithm development, and the validation of the results (McClain, 2009). Validation of sensor retrieved geophysical parameters with in-situ data helps to monitor the quality of sensor retrievals. Here, in-situ data assumed as ground truth and compared with OCM-1 data.

#### 3.1. SeaBASS Archive

SeaWiFS Bio-optical Archive and Storage System (SeaBASS), the publicly shared archive of in-situ oceanographic and atmospheric data maintained by the NASA Ocean Biology Processing Group (OBPG). The Global Ocean colour scientific community contributes to the archive through their timely cruises worldwide.

#### 3.2. Validation of OCM-1 Chlorophyll-a Concentration with SeaBASS

In-situ data provided by the SeaBASS covering the OCM-1 period is part of the Mediterranean Sea, Indian, and Pacific Oceans Transect (MIPOT) oceanographic campaign conducted in 2001. The ENEA (Italian Agency for New Technologies, Energy and the Environment) lidar fluorosensor (ELF), aboard the research vessel *Italica*, measured continuously surface chlorophyll-a concentrations during Italy–New Zealand and New Zealand–Italy transects from 13<sup>th</sup> November to 18<sup>th</sup> December 2001 and 28<sup>th</sup> February to 1<sup>st</sup> April 2002, respectively (Barbini et al 2004). The ship track passes through NIO from 23<sup>rd</sup> November to 27<sup>th</sup> November 2001 achieved after screening. In the above data 541 stations were covered in the area of interest, NIO along with the cruise dates are listed in **Table 5**. Out of 541 stations, 368 points/pixels are collocated with OCM-1 chlorophyll, unavailability of data due to cloud coverage, and issues related to data quality (**Figures 10 and 11**).

**Table 5:** Number of in-situ MIPOT cruise stations covered in the North Indian Ocean.

| Date | No. of stations covered NIO |
|------|-----------------------------|
|------|-----------------------------|

|                  |       |
|------------------|-------|
| 23 November 2001 | 93    |
| 24 November 2001 | 124   |
| 25 November 2001 | 144** |
| 26 November 2001 | 144** |
| 27 November 2001 | 36    |
| Total            | 541   |

\*\* ~ 6 measurements per hour

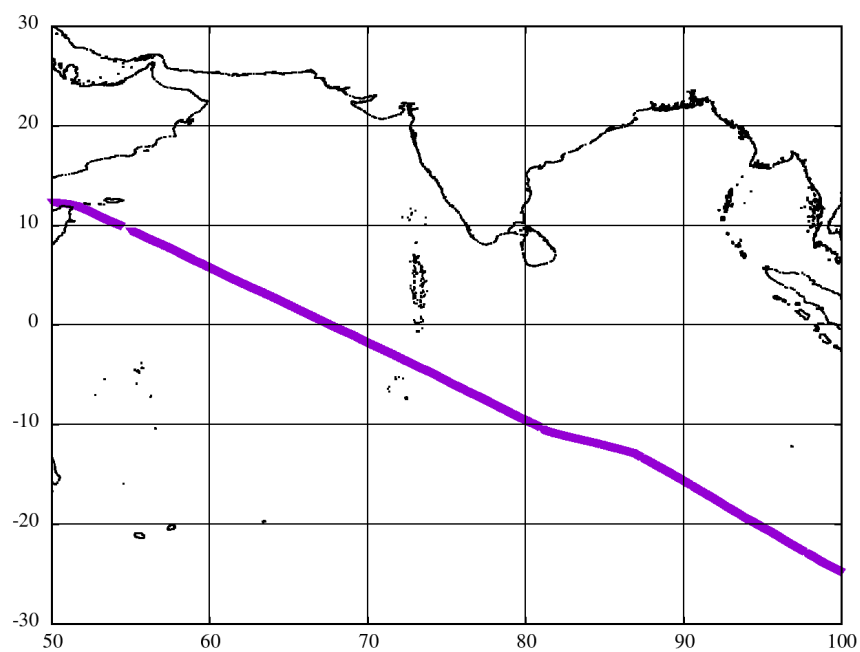


**Figure 10:** November 2001 MIPOT cruise track coverage over Indian ocean from SeaBASS archive

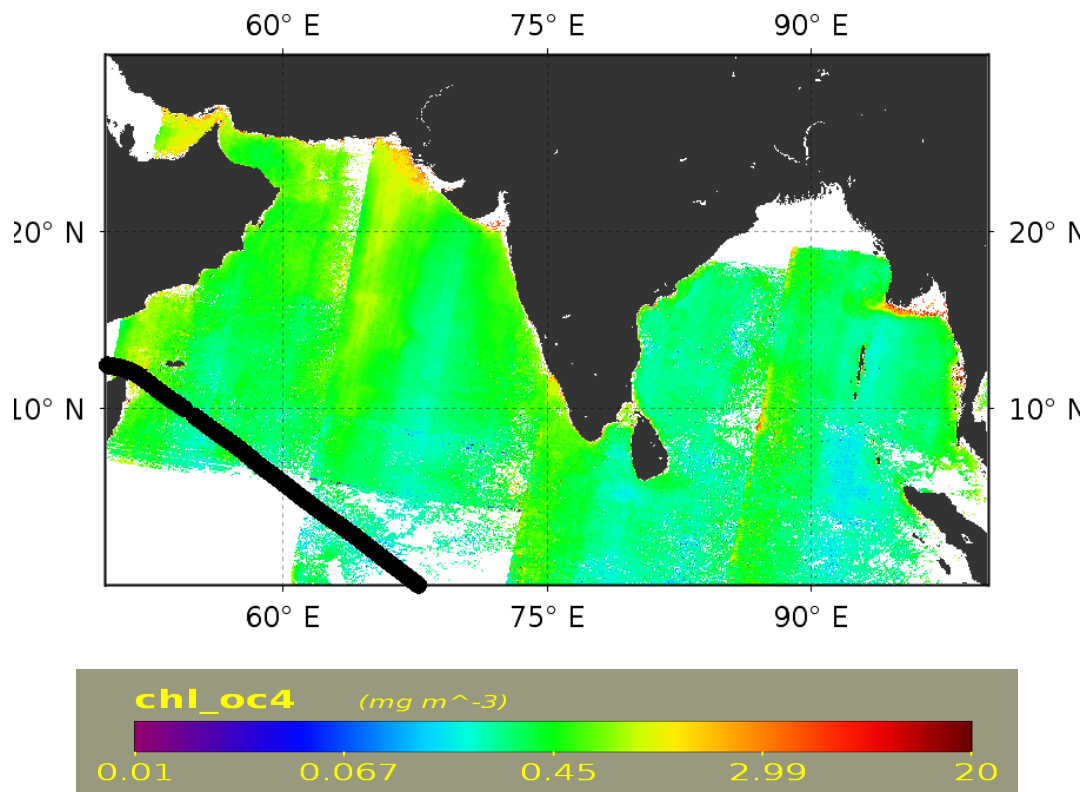
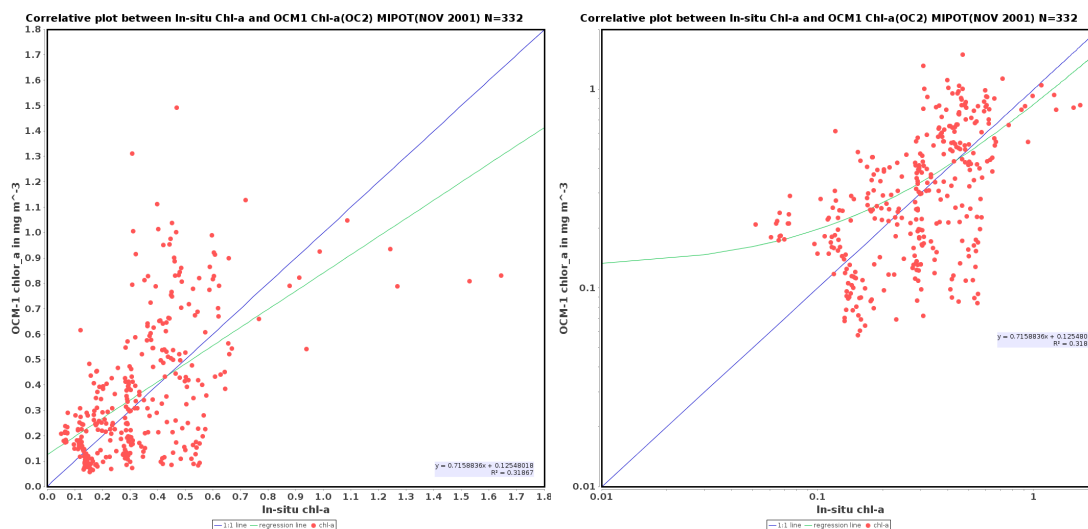


**Figure 11:** Ship track of MIPOT cruise imported on monthly chlorophyll (OC4) concentration ( $\text{mg}/\text{m}^3$ ) in November 2001 at 9 km resolution, the black line is showing the ship track.

SeaDAS provides a tool to compare satellite data with in-situ stations, it provides a scatter plot along with regression line and comparison statistics. Imported ship track as vector data on OCM-1 level-3 monthly mapped chlorophyll concentration and compared in-situ chlorophyll-a with OCM-1 OC2 and OC4 chlorophyll concentrations. Observed correlation ( $r^2$ ) 0.31 when in-situ chlorophyll-a concentration compared with OCM-1 chlorophyll (OC2 algorithm) and correlation ( $r^2$ ) 0.32 with chlorophyll (OC4) over 332 in-situ cruise stations (**Figure 12 and Table 7**). In the same way, the stations covered in individual consecutive five days (**Table 6**) compared with level-2 chlorophyll OC2 and OC4 products to evaluate the level-2 product quality. In a comparison of collocated pixels (**Figure 13**) on 23 November 2001, the good correlation observed ( $r^2 = 0.6$ ) but the slope is 2 units and the intercept is 0.07. Remaining days in level-2 chlorophyll comparison provided in **Annexure-II**. For the both OC2 and OC4 retrieved chlorophyll shown the same values over the collocated pixels level-2 and level-3 chlorophyll comparison, it conveys the same maximum  $R_{rs}$  ratio is picked up in both the OC2 and OC4 algorithms (**Figure 12 and 13**).

**Table 6:** Statistics showing the validation results of SeaBASS ins-situ data with OCM-1 chlorophyll concentration.

| Date            | Data Level                  | Number of in-situ stations | Number of pixels collocated | r <sup>2</sup> value | slope | intercept |
|-----------------|-----------------------------|----------------------------|-----------------------------|----------------------|-------|-----------|
| OC2 Chlorophyll | Level-3 data at 1 km binned | 541                        | 332                         | 0.31                 | 0.71  | 0.12      |
| OC4 Chlorophyll | Level-3 data at 1 km binned | 541                        | 332                         | 0.32                 | 0.61  | 0.23      |
| OC2 Chlorophyll | Level-2 data at 1 km binned | 144                        | 45                          | 0.68                 | 2.06  | 0.07      |
| OC4 Chlorophyll | Level-2 data at 1 km binned | 144                        | 45                          | 0.68                 | 2.06  | 0.07      |



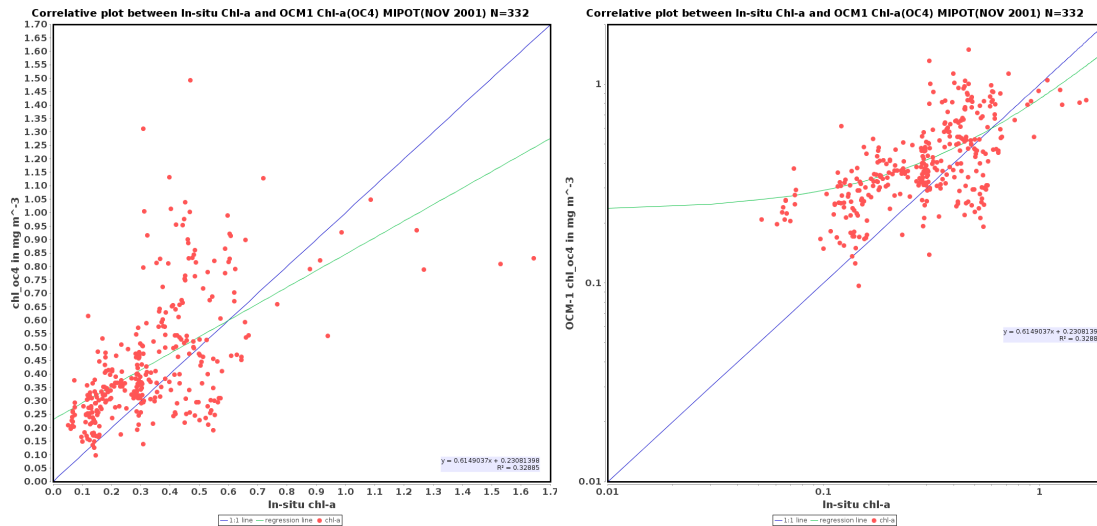


**Figure 12:** Correlative plot between in-situ chlorophyll-a and OCM-1 monthly OC2 chlorophyll in linear scale (top left) and logarithmic scale (top right) and OCM-1 OC4 chlorophyll in linear scale (bottom left) and logarithmic scale (bottom right) on November 2001.

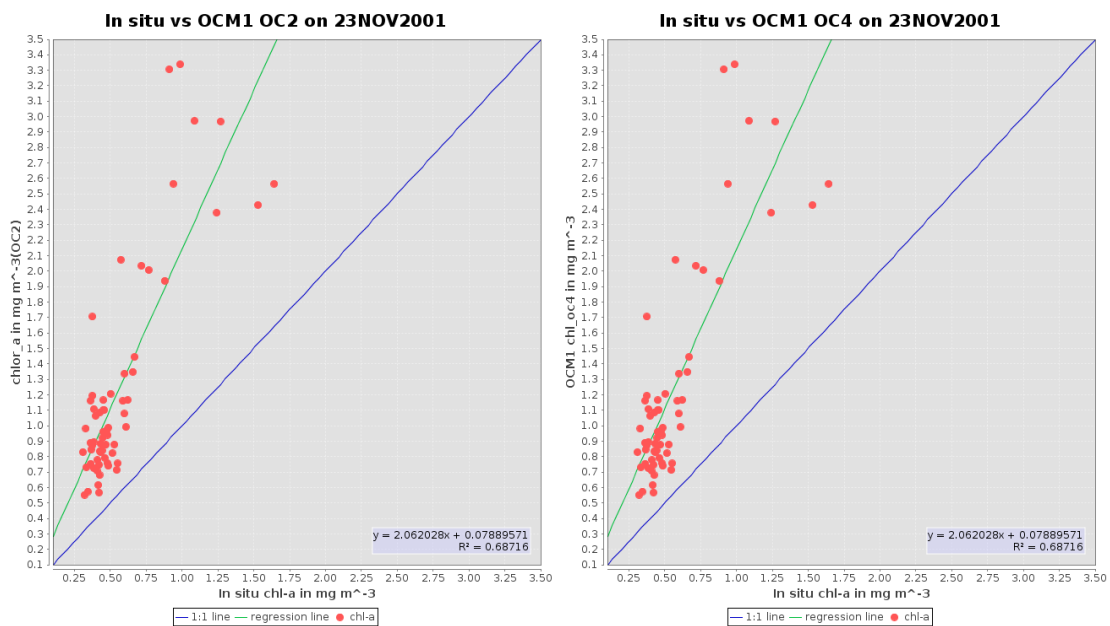


**Figure 13:** Correlative plot between in-situ chlorophyll-a with OCM-1 level-2 OC2 chlorophyll-a (left) and OCM-1 OC4 chlorophyll-a (right) respectively on 23 November 2001.

## 4. Future Scope of the Work

The present data for the two major geophysical products were generated for 15 years using standard OCS algorithms and uniform data format and quality as the



continuity mission of OCM-2. Any up-gradation in product quality by sensor calibration or advances in processing methodologies in terms of Rayleigh LUTs, aerosol models leads to reprocessing of the sensor for better retrieval. Improved products will be available to the users according to the new reprocessing version as per NASA/OBPG protocols update. The following are a few plans that will be addressed in sensor reprocessing over time.

- Chlorophyll algorithms can be updated to index-based ocean colour algorithms (OCI), or simultaneous usage of OC4 and OCI on weightage basis as adopted by MODIS-Aqua chlorophyll (O'Reilly et al 2000, Hu et al 2012)
- Ingestion of near real-time meteorological parameters to depict the actual/original field conditions of atmosphere and ocean surface (Satyadev et al 2011) at the time of acquisition.
- Improvement in OCM-1 TOA radiances by adopting inter-sensor calibration with respect to SeaWiFS
- Addressing overestimations of  $R_{rs}$  and chlorophyll at the edge of the scenes
- Regional aerosol model for aerosol correction by understanding aerosol properties over NIO

## 5. References

1. R. R Navalgund, A. S. Kiran Kumar, Ocean colour Monitor (OCM) on Indian Remote Sensing Satellite IRS-P4, <http://www.ioccg.org/reports/ocm/ocm.html> (1999).
2. HU Solanki, RM Dwivedi., Ocean colour Applications to Ocean Biology, ISRO Scientific Report - VOL-II; IRS-P4/SATCORE/SAC/RESIPA/MWRG/SR/22/2003; ISRO: Ahmedabad, India (2003).
3. Chauhan, P., and R. R., Navalgund, Ocean Colour Monitor (OCM) onboard OCEANSAT-2 mission. <https://www.ioccg.org/sensors/OCM-2.pdf> (2009).
4. Gordon, H. R. Atmospheric correction of ocean colour imagery in the Earth-observing system era. *J. Geophys. Res. Atmos.* 102, 17081–17106 (1997).
5. André, J.-M. & Morel, A. Atmospheric corrections and interpretation of marine radiances in CZCS imagery, revisited. *Oceanol.Acta.*14:3-22 (1991).
6. Hovis, W. A. & Leung, K. C., Remote Sensing of Ocean colour. *Opt. Eng.* 16, 332–339 (1977).
7. Wang, M., Rayleigh radiance computations for satellite remote sensing: accounting for the effect of sensor spectral response function. *Opt. Express* 24, 12414 (2016).

8. Gordon, H. R. & Wang, M., Retrieval of water-leaving radiance and aerosol optical thickness over the oceans with SeaWiFS: a preliminary algorithm. *Appl. Opt.* 33, 443 (1994).
9. Ahmad, Z. & Fraser, R. S., An iterative radiative transfer code for ocean-atmosphere systems. *Journal of the Atmospheric Sciences* vol. 39 656–665 (1982).
10. Gordon, H. R., Brown, J. W. & Evans, R. H. Exact Rayleigh scattering calculations for use with the Nimbus-7 Coastal Zone colour Scanner. *Appl. Opt.* 27, 862 (1988).
11. Wang, M. A refinement for the Rayleigh radiance computation with variation of the atmospheric pressure. *Int. J. Remote Sens.* 26, 5651–5663 (2005).
12. Siegel, D. A., Wang, M., Maritorena, S. & Robinson, W. Atmospheric correction of satellite ocean colour imagery: the black pixel assumption. *Appl. Opt.* 39, 3582 (2000).
13. Ahmad, Z., New aerosol models for the retrieval of aerosol optical thickness and normalized water-leaving radiances from the SeaWiFS and MODIS sensors over coastal regions and open oceans. *Appl. Opt.* 49, 5545–5560 (2010).
14. Wang, M. & Bailey, S. W., Correction of sun glint contamination on the SeaWiFS ocean and atmosphere products. *Appl. Opt.* 40, 4790 (2001).
15. Thuillier, G. et al. The solar spectral irradiance from 200 to 2400 nm as measured by the SOLSPEC spectrometer from the ATLAS and EURECA missions. *Sol. Phys.* 214, 1–22 (2003).
16. M. Wang, The Rayleigh lookup tables for the SeaWiFS data processing: Accounting for the effects of ocean surface roughness, *Int. J. Remote Sens.* 23, 2693–2702 (2002).
17. B. A. Franz, S. W. Bailey, P. J. Werdell, and C. R. McClain, Sensor-independent approach to the vicarious calibration of satellite ocean colour radiometry, *Appl. Opt.* 46, 5068–5082 (2007).
18. C. D. Mobley, J. Werdell, B. Franz, Z. Ahmad, and S. Bailey, Atmospheric Correction for Satellite Ocean colour Radiometry, NASA Tech. Memo. 2016–21755, 1–73 (2016).
19. J. E. O'Reilly, S. Maritorena, B. G. Mitchell, D. A. Siegel, K. L. Carder, S. A. Garver, M. Kahru, and C. McClain, Ocean colour chlorophyll algorithms for SeaWiFS, *J. Geophys. Res. Ocean.* 103, 24937–24953 (1998).
20. Mickelson, Wang, Statistical evaluation of satellite ocean colour data retrievals, *Remote Sensing of Environment* 237 -111601 (2020).
21. Barnes, B.B., Hu, C., Dependence of satellite ocean colour data products on viewing angles: a comparison between SeaWiFS, MODIS, and VIIRS. *Remote Sens. Environ.* 175, 120–129 (2016).
22. McClain, C.R., A decade of satellite ocean colour observations. *Annu. Rev. Mar. Sci.* 1, 19–42 (2009).

23. R. Barbini, F. Colao, L. De Dominicis, R. Fantoni, L. Fiorani, A. Palucci And E. S. Artamonov, Analysis of simultaneous chlorophyll measurements by lidar fluorosensor, MODIS and SeaWiFS. INT. J. REMOTE SENSING, VOL .25, NO. 11, 2095-2110 (2004).
24. W. D. Robinson, B. A. Franz, F. S. Patt, S. W. Bailey, and P. J. Werdell, Masks and flags updates, NASA Goddard Space Flight Center, Greenbelt, MD, pp. 34–40, SeaWiFS Postlaunch Technical Report Series, NASA Tech. Memo. 2003-206892 (2003).
25. Wang, Menghua & Shi, Wei., Cloud Masking for Ocean colour Data Processing in the Coastal Regions. Geoscience and Remote Sensing, IEEE Transactions on. 44. 3196 - 3105. 10.1109/TGRS.2006.876293 (2006).
26. NASA Ocean colour SeaWiFS ocean colour reprocessing 2018.0. <https://oceancolour.gsfc.nasa.gov/reprocessing/r2018/seawifs/> (2018).
27. Chauhan, P., Mohan, M. & Nayak, S., Comparative analysis of ocean colour measurements of IRS-P4 OCM and SeaWiFS in the Arabian Sea. IEEE Transactions on Geoscience and Remote Sensing vol. 41 922–926 (2003).
28. Dash, P., Walker, N., Mishra, D., D'Sa, E. & Ladner, S., Atmospheric correction and vicarious calibration of oceansat-1 ocean colour monitor (OCM) data in coastal case 2 waters. Remote Sens. 4, 1716–1740 (2012).
29. SeaWiFS Project - Spacecraft and Sensor Overview. <https://oceancolour.gsfc.nasa.gov/SeaWiFS/SEASTAR/SPACECRAFT.html>.
30. IOCCG Report Series 01: Minimum Requirements for an Operational, Ocean-Colour Sensor for the Open Ocean. Edited by: André Morel. vol. 01 (1998).
31. O'Reilly, J.E., & 24 co-authors., SeaWiFS Postlaunch Calibration and Validation Analyses, Part 3. NASA Tech. Memo. 2000-206892, Vol. 11, S.B. Hooker and E.R. Firestone, Eds., NASA Goddard Space Flight Center, 49 pp, (2000).
32. Hu, C., Lee, Z., & Franz, B., Chlorophyll-a algorithms for oligotrophic oceans: A novel approach based on three-band reflectance difference. Journal of Geophysical Research, 117(C1). doi: 10.1029/2011jc007395 (2012).

## APPENDIX - I

**Table A1:** Few parameters from metadata of a product (dataset/variable)

| Attribute Name | Example                             |
|----------------|-------------------------------------|
| product_name   | "SMI_1KM_OC2_1999_AUG.nc"           |
| instrument     | "OCM"                               |
| title          | "OCM Level-3 Standard Mapped Image" |

|                                  |   |
|----------------------------------|---|
| <b>Project</b>                   | "Ocean Biology Processing Group<br>(NASA/GSFC/OBPG)"  |
| <b>platform</b>                  | "IRS-P4"  |
| <b>temporal_range</b>            | "month"   |
| <b>map_projection</b>            | "Equidistant Cylindrical"   |
| <b>northernmost_latitude</b>     | 30.f  |
| <b>southernmost_latitude</b>     | -30.f   |
| <b>westernmost_longitude</b>     | 50.f  |
| <b>easternmost_longitude</b>     | 100.f   |
| <b>latitude_units</b>            | "degrees_north"   |
| <b>longitude_units</b>           | "degrees_east"  |
| <b>geospatial_lon_resolution</b> | 1.2f  |
| <b>geospatial_lat_resolution</b> | 1.2f  |
| <b>spatialResolution</b>         | "1.20 km"   |
| <b>number_of_lines</b>           | 5760  |
| <b>number_of_columns</b>         | 4800  |
| <b>l2_flag_names</b>             | "ATMFAIL, LAND, HILT, HISATZEN, STRAYLIGHT, CLDICE, COCCOLITH, LOWLW, CHLWARN, CHLFAIL, NAVWARN, MAXAERITER, ATMWARN, HISOLZEN, NAVFAIL, FILTER, HIGLINT" |
| <b>Measure</b>                   | "Mean"  |
| <b>Conventions</b>               | "CF-1.6"  |
| <b>standard_name_vocabulary</b>  | "NetCDF Climate and Forecast (CF) Metadata Convention"  |
| <b>processing_level</b>          | "L3 Mapped"   |
| <b>Keywords</b>                  | "Oceans > Ocean Chemistry > Chlorophyll; Oceans > Ocean Optics > Ocean colour"  |

**Table A2:** Few parameters from metadata of a product (attribute)

| <b>Attribute Name</b> | <b>Example</b>  |
|-----------------------|---|
| <b>Long_name</b>      | "Chlorophyll Concentration, OC2 Algorithm" ;                |
| <b>units</b>          | "mg m <sup>-3</sup> "                                       |
| <b>standard_name</b>  | "mass_concentration_chlorophyll_concentration_in_sea_water" |
| <b>_FillValue</b>     | -32767.f  |
| <b>valid_min</b>      | 0.001f  |
| <b>valid_max</b>      | 100.f   |

**Table A4:** Quality flags thresholds in l2gen processing

| <b>Flag</b>         | <b>Threshold</b> | <b>Flag</b>         | <b>Threshold</b> |
|---------------------|------------------|---------------------|------------------|
| <b>sunzen</b>       | 70.000           | <b>tauamax</b>      | 0.300            |
| <b>satzen</b>       | 60.000           | <b>wsmax</b>        | 12.000           |
| <b>glint_thresh</b> | 0.005            | <b>nlwmin</b>       | 0.150            |
| <b>epsmax</b>       | 1.350            | <b>cloud_thresh</b> | 0.027            |
| <b>epsmin</b>       | 0.800            |                     |                  |

**Table A5:** Description of quality flags in Level 2 processing

| <b>Flag name</b> | <b>Bit number</b> | <b>Flag value</b> | <b>Flag Description</b>                                       |
|------------------|-------------------|-------------------|---|
| ATMFAIL          | 00                | 1                 | Atmospheric correction failure                                |
| LAND             | 01                | 2                 | Pixel is on land  |
| PRODWARN         | 02                | 4                 | One or more product algorithms generated a warning            |
| HIGLINT          | 03                | 8                 | LGN > 0.005   |
| HILT             | 04                | 16                | Observed radiance very high or saturated in one or more bands |
| HISATZEN         | 05                | 32                | SATZEN > 60   |
| COASTZ           | 06                | 64                | Pixel is in shallow water                                     |
| Spare            | 07                | 128               |   |
| STRAYLIGHT       | 08                | 256               | Probable stray light contamination                            |
| CLDICE           | 09                | 512               | Rho(865) > 0.027  |
| COCCOLITH        | 10                | 1024              | Coccolithophores detected                                     |
| TURBIDW          | 11                | 2048              | Rrs(670) > 0.0012 /sr   |
| HISOLZEN         | 12                | 4096              | SOLZEN > 70   |
| Spare            | 13                | 8192              |   |
| LOWLW            | 14                | 16384             | nLw(555) > 0.15   |

|            |    |            |   |
|------------|----|------------|---|
| CHLFAIL    | 15 | 32768      | chl <0.0  |
| NAVWARN    | 16 | 65536      | Navigation quality is suspect   |
| ABSAER     | 17 | 131072     | Absorbing Aerosols determined   |
| Spare      | 18 | 262144     |   |
| MAXAERITER | 19 | 524288     | Maxaeriter 10 reached   |
| MODGLINT   | 20 | 1048576    | $L_{GN} > 0.0001$   |
| CHLWARN    | 21 | 2097152    | Chl <0 (or)Chl>100  |
| ATMWARN    | 22 | 4194304    | Eps < 0.85 (or) eps > 1.35  |
| Spare      | 23 | 8388608    |   |
| SEAICE     | 24 | 16777216   | Probable sea ice contamination  |
| NAVFAIL    | 25 | 33554432   | Navigation failure  |
| FILTER     | 26 | 67108864   | Pixel rejected by user-defined filter OR Insufficient data for smoothing filter |
| Spare      | 27 | 134217728  |   |
| BOWTIEDEL  | 28 | 268435456  | Deleted off-nadir, overlapping pixels (VIIRS only)                              |
| HIPOL      | 29 | 536870912  | Degree of polarization > 0.5  |
| PRODFAIL   | 30 | 1073741824 | Failure in any product  |
| Spare      | 31 | 2147483648 |   |

source: <https://oceancolour.gsfc.nasa.gov/atbd/ocl2flags/>

**Table A6:** Sensor Specifications For SeaWiFS comparative with OCM-1

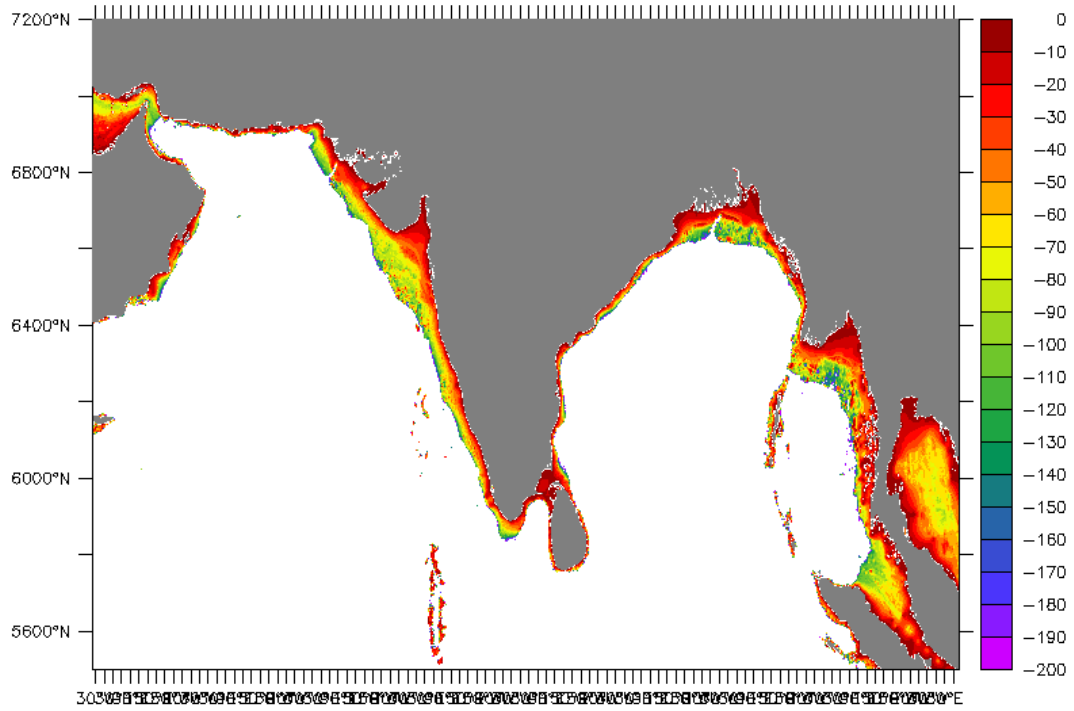


**Figure A1:** Depth (surface is zero) in the North Indian Ocean from 0 to 200 m

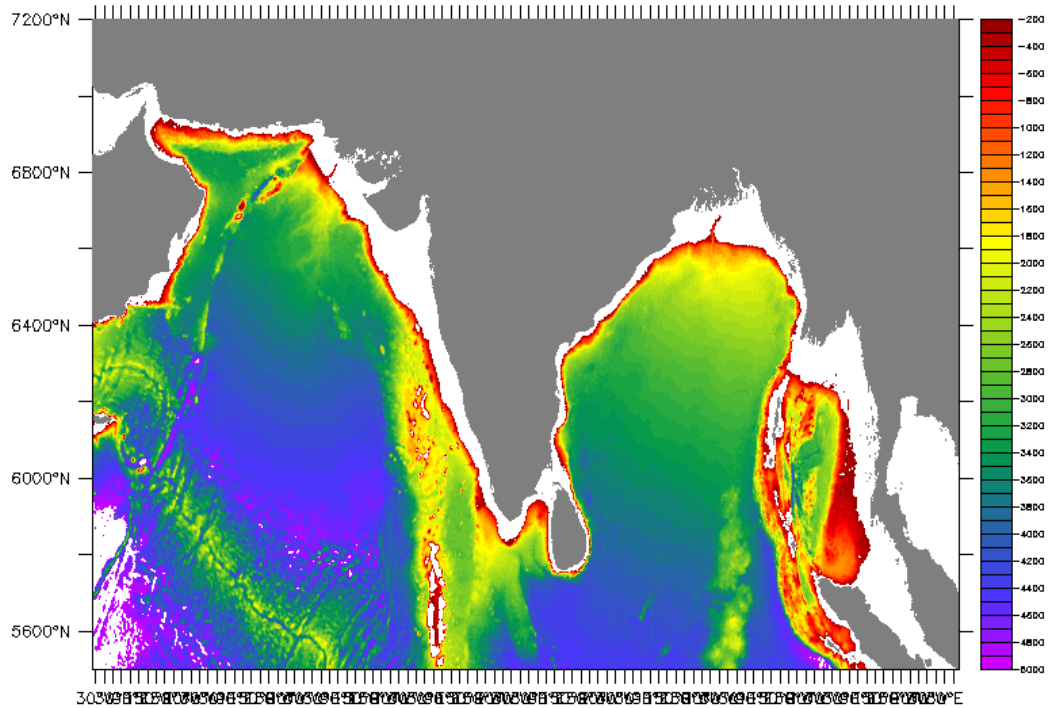


**Figure A2:** Depth in North Indian Ocean from 200 m to 5000 m  
 (\*negative values shows below Mean Sea Level in m)

## **APPENDIX - II**

## Geo-physical products

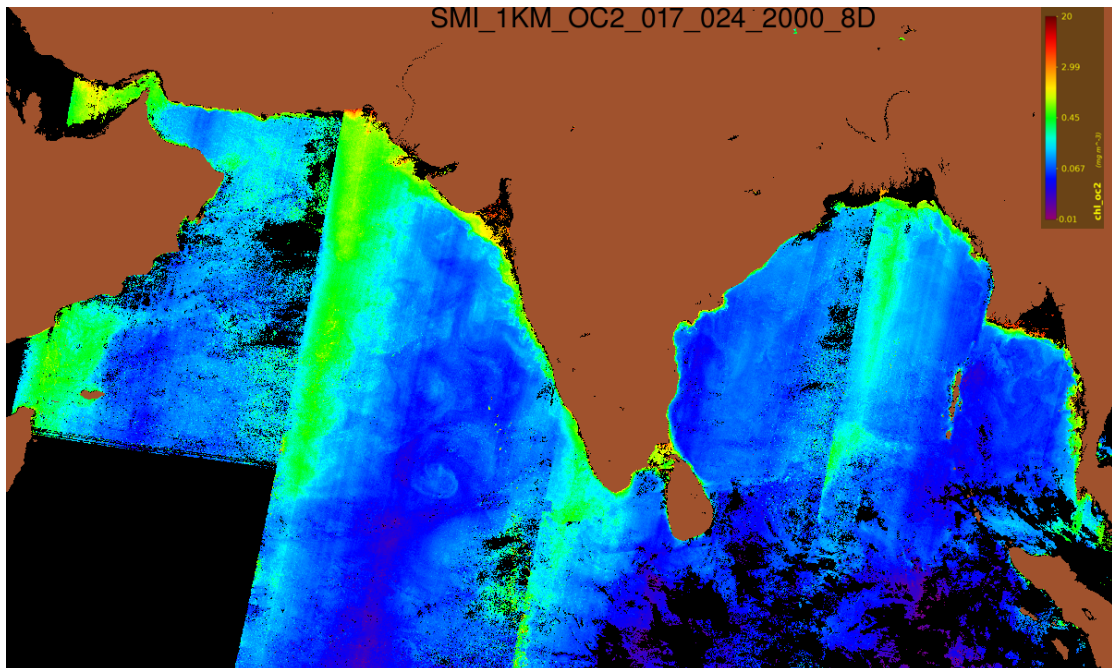


**Figure A3:** Chlorophyll (OC2) concentration (mg/m<sup>3</sup>) 8-day composite map over NIO from OCM-1 on 17 to 24 January 2000 at a spatial resolution of 1 km

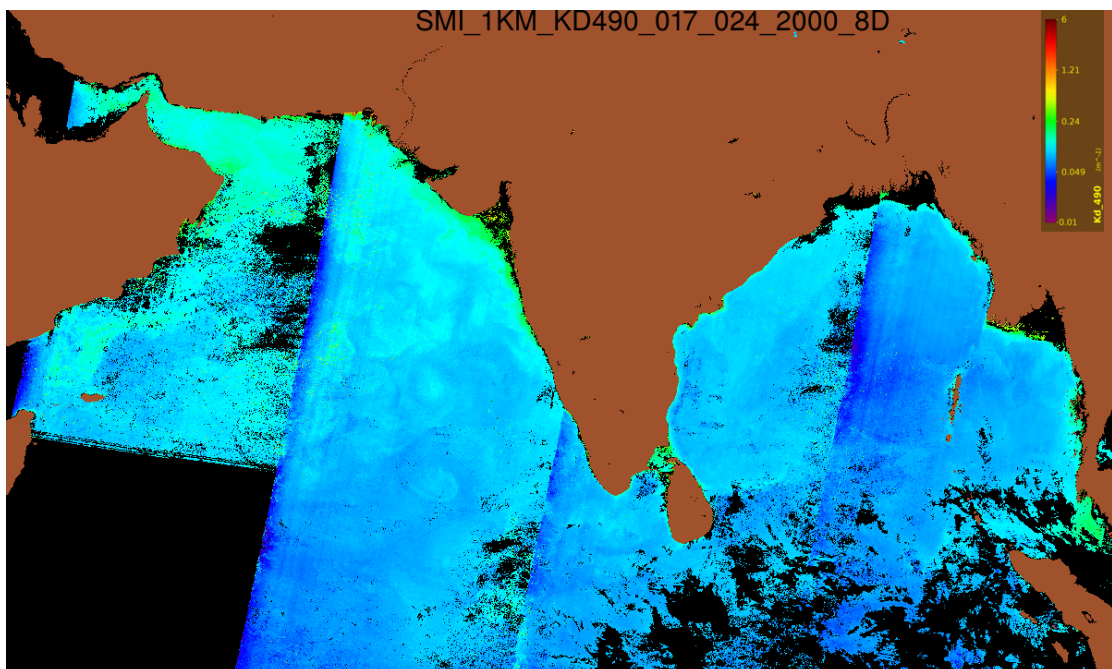


**Figure A4:** Diffuse attenuation coefficient (/m) 8-day composite map over NIO from OCM-1 on 17 to 24 January 2000 at a spatial resolution of 1 km



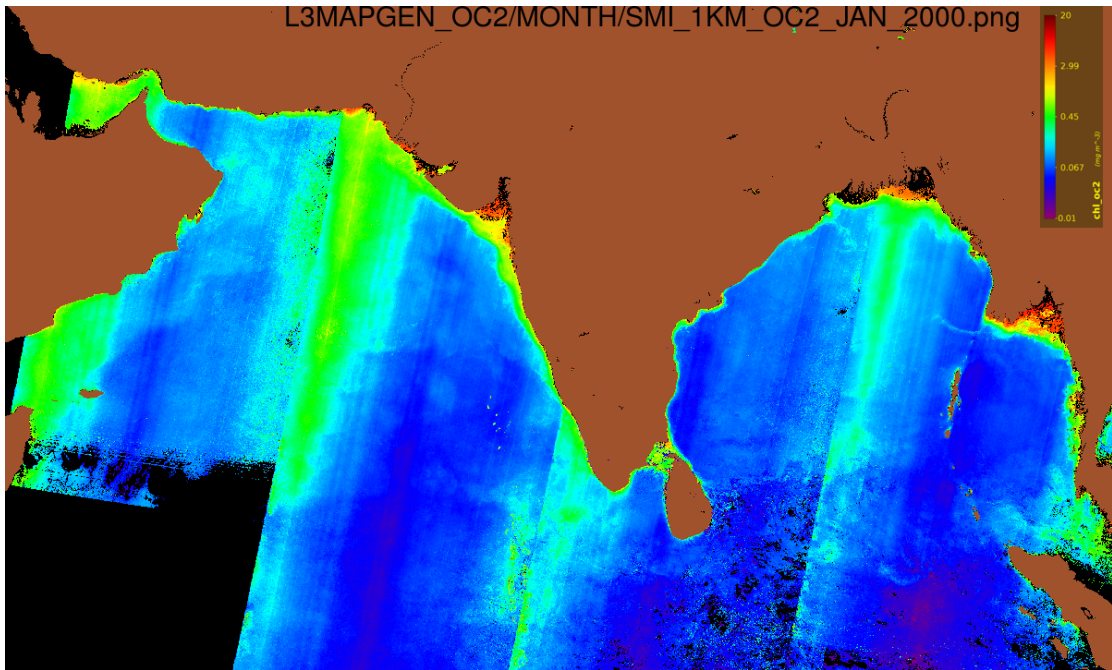


**Figure A5:** Chlorophyll (OC2) concentration (mg/m<sup>3</sup>) monthly map over NIO from OCM-1 on January 2000 at a spatial resolution of 1 km

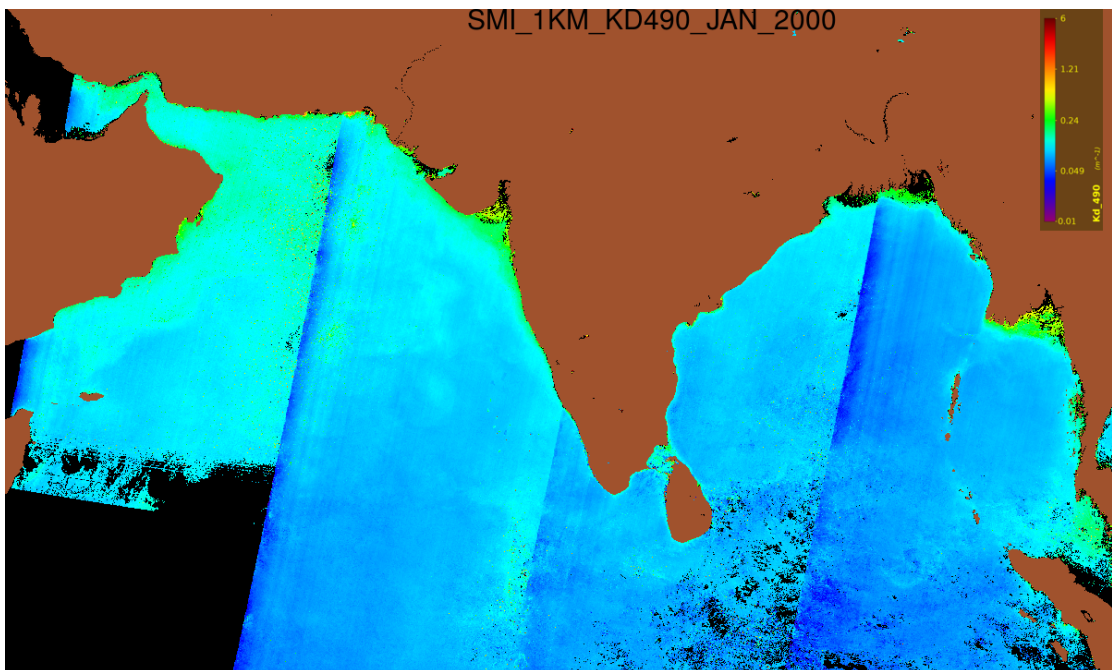


**Figure A6:** Diffuse attenuation coefficient (/m) monthly map over NIO from OCM-1 on January 2000 at a spatial resolution of 1 km

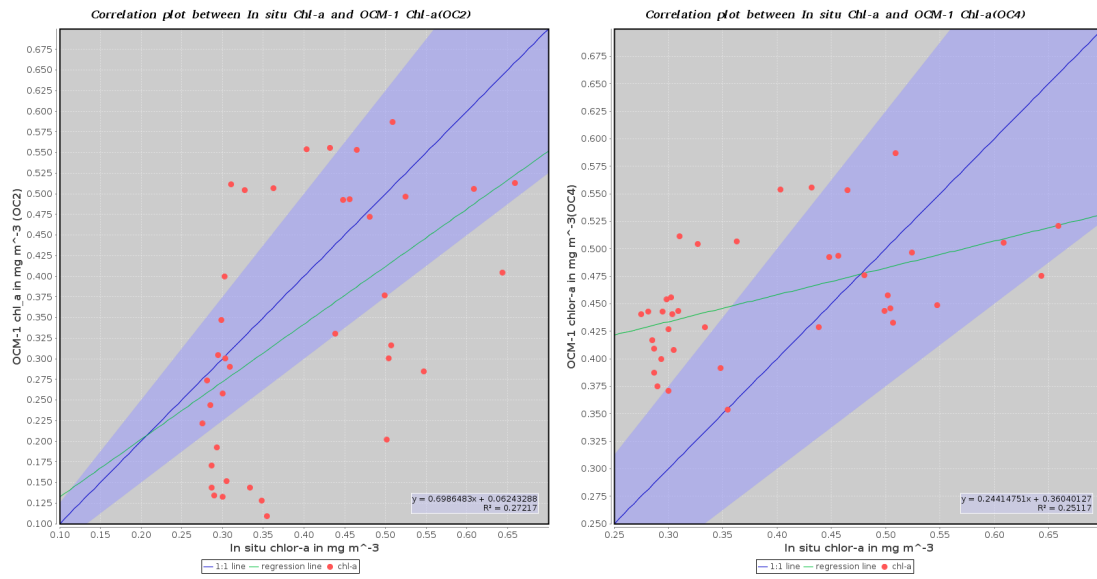


**Figure A7:** Correlative plot between in-situ chlorophyll-a with OCM-1 level-2 OC2 chlorophyll-a (left) and OCM-1 OC4 chlorophyll-a (right) respectively on 25 November 2001.